Consiglio Nazionale delle Ricerche

ISTITUTO DI ELABORAZIONE DELLA INFORMAZIONE

PISA

SPACE TIME FINITE ELEMENTS FOR PARABOLIC AND HYPERBOLIC OPERATORS

A. Cella, M. Lucchesi, G. Pasquinelli

Nota Interna B77-17

Novembre 1977

SPACE TIME FINITE ELEMENTS FOR PARABOLIC AND HYPERBOLIC OPERATORS

A. Cella[+], M. Lucchesi[++], G. Pasquinelli[++]

[+]Istituto di Elaborazione dell'Informazione, C.N.R., Pisa

[++]CNUCE, Istituto del C.N.R., Pisa

ABSTRACT

Differential problems of parabolic and hyperbolic type are presented in the weak (variational) formulation across the space and time variables.

A discrete approximation is performed using linear "shape" functions in space and time. It is shown how, by setting the appropriate conditions on the test function v, the size of the discrete problem reduces to the total number of variables in space, as for Galerkin method.

The numerical performance of space-time elements is compared to "optimal" Galerkin algorithms, in a series of test problems where the analytic solution is known.

For parabolic problems where f is independent of t, space-time elements hold the line with the optimal ($\theta = 2/3$) Galerkin, showing some allergy, however, to discontinuities between initial and boundary conditions. For parabolic problems where f depends on t, the space-time elements perform much better.

For hyperbolic problems (with f dependent or not from time) the space-time elements show a surprising accuracy: they stick to the analytic solution while Galerkin (central differences) runs out of phase or blows out for numerical instability.

1. INTRODUCTION

Since the early applications of the finite element method to heat transfer or to elastodynamics [12], it seemed desirable to blend the space and time variables into a unique finite element formulation, rather than mixing finite elements (in space) and finite differences (in time), as in the universally used Faedo-Galerkin approach.

Implementations of the space-time element technique, however, have been scarce [5] due, partly, to the lack of support from a comprehensive theory and, to a greater extent, to the blow up in size of the associated numerical problem. When the nodal values of the solution become simultaneously unknown at all time steps, the problem size (and the bandwidth) of the matrix may grow by an order of magnitude.

A comprensive theory of the "equations of evolution" was, indeed, existing, and had reached its full bloom in the work of Lions and Magenes [2]. There, the weak formulation for ellyptic operators [1] was extended, via time integration, to parabolic and to hyperbolic problems. The regularity of the solution was proved under mildly restrictive conditions on the initial and on the boundary conditions of the problems. A first attempt at extracting from the theory a numerical algorithm for the heat transfer problem was made by the first author and M. Morandi Cecchi [3,4]. The reduction of the numerical problem to Galerkin size was achieved. However, the misfortunate choice of the test cases lead to doubts as to whether space-time elements were competitive with the Gaerkin method. A subsequent attempt by the first two authors with the wave propagation problem didnt lead to any evidence, either way [10].

Finally, a restart from the basic theory, a careful analysis of the algorithms, and ample numerical testing have brought to the conclusion that space-time elements are superior, accuracy-wise (at the same computational conditions) to the optimal Galerkin algorithms. The superiority becomes striking either with coarse time steps or with time-dependent f.

The range of testing is confined to one-dimensional problems, but is sufficiently articultate (the authors believe) to prototype the behaviour of multidimensional problems.

Further developments are to be seen.

2. WEAK FORMULATION FOR PARABOLIC PROBLEMS

Let Ω be an open bounded domain in R^n, and let $\partial\Omega$ be its boundary. Let $I =]o,T[$ be the open time interval, and let $C = \{(x,t) \in R^{n+1} \mid x \in \Omega, t \in I\}$ be the open cylinder in the space--time domain.

Let A be a 2^{nd} order partial differential operator defined as

(1) $$A = -\sum_{i,j=o}^{n} D_j(a_{ij}(x,t)D_i); \quad (D_i = \frac{\partial}{\partial x_i}; \ D_o u = u)$$

where $a_{ij}(x,t)$ are real valued functions defined on $\bar{C}$ and there sufficiently regular.

Assuming that A is ellyptic with respect to x, uniformly so with respect to t, i.e.

(2) $$\sum_{i,j=oK}^{n} a_{ij}\,\varrho^i\,\varrho^j \geq \nu\|\varrho\|^2 \quad , \ \nu>o, \quad \varrho\in R^n, \ (x,t) \in C$$

then, it is known from the literature [1], that the family of bilinear forms defined on the Sobolev space $H^1(\Omega)$

(3) $$a(t;u,v) = \int_\Omega \sum_{i,j=0}^{n} a_{ij}(x,t)D_i\, u\, D_j\, v\, dx$$

is weakly cohercive on $H_o^1(\Omega)$ for every $t\in I$, i.e. that real constants $\alpha>o$, $\lambda\geq o$ exist such that

(4) $a(t;u,u) \geq \alpha \|u\|^2_{H^1(\Omega)} - \lambda \|u\|^2_{L^2(\Omega)}$

for every $t \in I$ and for every $u \in H^1_o(\Omega)$.

Assuming the regularity of the coefficients $a_{ij}(x,t)$, the family of bilinear forms is bounded in $H^1(\Omega)$, i.e.

(5) $|a(t;u,v)| \leq M \|u\|_{H^1(\Omega)} \|v\|_{H^1(\Omega)}, \quad M > o$

for every $t \in I$.

Under all the previous assumptions it can be proved [2] that:

given $u_o(x) \in L^2(\Omega)$ and $f(x,t) \in L^2(C)$, there exists a unique function $u(x,t) \in L^2(O,T;H^1_o(\Omega))$ such that

(6) $\int_o^T (a(t;u,v) - (u,\dot{v})_{L^2(\Omega)})dt = \int_o^T (f,v)_{L^2(\Omega)} dt + (u_o, v(o))_{L^2(\Omega)}$

for every $v \in W_o(O,T)$ (1); in addition

(7) $\|u\|_{L^2(o,T;H^1_o(\Omega))} \leq C \{ \|f\|_{L^2(C)} + \|u_o\|_{L^2(\Omega)} \}$

Equation (6) can be written in the form

(8) $\int_C (\sum_{i,j=0}^n a_{ij}(x,t)\, D_i u D_j v)\, dx\, dt - \int_C (u \cdot \dot{v}) dx\, dt =$

$\int_C (f.v) dx\, dt + \int_\Omega (u_o . v(o)) dx$

---

(1) We call $W_o(O,T)$ the space of real functions $v(x,t)$, defined on C, such that $v \in L^2(O,T;H^1_o(\Omega))$, $\dot{v} \in L^2(C)$, $v(T) = O$

Equation (8) represents the weak formulation for a linear parabolic problem , as it can be proved [2] that:

a) $\langle Au+\dot{u},v\rangle = (f,v)_{L^2(C)}$ $\quad ,v\in C_0^{\infty}(C)$

therefore (in the sense of the distributions on C):

$$Au+\dot{u} = f$$

b) $\lim_{t\to o} (u(x,t),v(x))_{L^2(\Omega)} = (u_o(x),v(x))_{L^2(\Omega)}$ $, v\in L^2(\Omega)$

therefore $u(x,t)$ tends, for t going to 0, to $u_o(x)$,

weakly in $L^2(\Omega)$;

c) $u(x,t) = o$ for $(x,t)\in \delta\Omega XI$ $\quad$,as $u(x,t)\in L^2(O,T;H_o^1(\Omega))$

3. SPACE-TIME APPROXIMATION (PARABOLIC)

For sake of simplicity, we make reference to the following one-dimensional problem, that prototypes the propagation of heat in a wall

Problem PP

(9.1) $\quad -ku_{xx}+c\dot{u} = f(x,t) \qquad (x,t)\in C \qquad k,c$ real constants

(9.2) $\quad u(x,o)=u_o(x) \qquad x\in]o,b[$

(9.3) $\quad u(0,t) = u(b,t) = 0 \qquad t\in [o,T]$

where it is assumed that

$f\in L^2(o,T;L^2(o,b))$; $u_o\in L^2(o,b)$; $u\in L^2(o,T;H_0^1(o,b))$

The weak formulation (8) applied to problem (9) gives

(10) $\quad k((u_x,v_x)) - c((u,\dot{v})) = ((f,v)) + c\,(u_o,v_o) \qquad v\in W_0(O,T)$

where $((\,,)) = \int_o^T \int_o^b (.)dx\, dt$; $v_o = v(x,o)$; $(\,,) = \int_o^b (.)\, dx$

The domain $[0,b] \times [0,T]$ is partitioned into a finite number of elements spanning the space-time subdomains $[o,a]\times[o,\tau]$ in element-local coordinates. Inside the element the unknown function $u(x,t)$ is approximated by a bilinear function

(11) $\underline{u}(x,t) \simeq (1,x,t,xt)\,\underline{\alpha} = \underline{p}\,\underline{\alpha}$

where the parameters $\underline{\alpha} = N\underline{u}$ are represented as a function of the nodal values $\underline{u}$ of $u(x,t)$.

The approximating functions in $\underline{p}$ can be derived with respect to x and to t, thus giving.

(12) $\underline{u} \simeq \underline{p}N\underline{u}$; $u_x \simeq \tilde{\underline{p}}N\underline{u}$; $\dot{u} \simeq \hat{\underline{p}}N\underline{u}$

The same approximation applies to v. Introducing (12) into (10), and assembling over the elements the resulting discrete equations, one obtains

(13) $u^T K_x \underline{v} - \underline{u}^T K_t \underline{v} = \underline{f}F\underline{v} + u_o Q \underline{v}_o$

Where the expressions for K_x, K_t, F, N are given in Appendix 1. On the left hand side of eq. (13) the matrices K_x, K_t can be consolidated into $K = K_x - K_t$; the equations are partitioned into two blocks, referencing with index 1 the terms related to time t=o, and with index 2 the terms related to $t=\tau$; thus

(14) $\underline{u} = \begin{Bmatrix} \underline{u}_1 \\ \underline{u}_2 \end{Bmatrix} \begin{matrix} t=o \\ t=\tau \end{matrix}$; $\underline{u}_o = \begin{Bmatrix} \underline{u}_1 \\ o \end{Bmatrix}$

Notice that from (6) the "test" function v annihilates for $t = \tau$, therefore.

(15) $\underline{v} = v_o = \begin{Bmatrix} \underline{v}_1 \\ o \end{Bmatrix}$

Introducing (14) and (15) into (13) one obtains

(16) $\underline{u}_1 K_{11} \underline{v}_1 + \underline{u}_2 K_{21} \underline{v}_1 = \underline{f} F_1 \underline{v}_1 + \underline{u}_1 Q_{11} \underline{v}_1 \qquad \underline{v}_1 \in R^n$

eliminating $\underline{v}_1$, carrying the term with $\underline{u}_1$ on the right hand side, and trasposing the equations, one finally obtains

(17) $K_{21}^T \underline{u}_2 = F_1^T f + Q_{11}^T \underline{u}_1 - K_{11}^T \underline{u}_1$

Solving equation (17) in $\underline{u}_2$ gives the required nodal values $\underline{u}_2$ of the unknown function u at the time $t=\tau$. The procedure can iterate through any number of time steps. A few remarks:

a. - Equation (17), in its form, is not specifically related to the one-dimensional problem PP, but is the general expression of the space-time approximation to parabolic problems: it would have the same form in a higher order domain, or with a higher order approximation (provided hermitian polynomials are used, where the nodes are allocated, symmetrically, either at t=o or at $t=\tau$).

b. - The size is the same as for Galerkin method, i.e. the number of nodal variables at time t=o. We dont have here the blow-up of the size of the numerical problem to the full space-time dimensions, as in alternative approaches (see [5]).

c. - The matrix K_{12}^T is symmetric when linear approximation is used, regardless of the size of the domain; it could become non symmetric, though, with higher order approximation.

Therefore, solving a parabolic problem with the space-time finite element approximation implies the same computational effort, at each step, as with Galerkin method. The choice of either procedure rests solely on their relative accuracy. The following numerical tests try to make the point.

Notice that numerical stability is not of concern here, as Galerkin method is unconditionally stable for parabolic problems, and space-time elements are presumed (but not proved) to be so, from numerical evidence.

4. NUMERICAL TESTS (PARABOLIC)

A set of one-dimensional problems was selected to test the numerical accuracy of space-time elements against the "optimal" Galerkin method ($\vartheta = 2/3$, see for instance [6,7,8]). The comparison is made using the same, fix, discretization in space (n=9, providing adequate accuracy in space) and with the same, variable, time step; the test is carried through nine time steps. The analytic solution is known for all test problems; the error is measured in the L^2 norm:

$$\|e\|_L = \frac{1}{n} \sum_{i=1}^{n} |u_n(x_i) - u(x_i)| / |u(x_i)| \times 100 \qquad (18)$$

at every time step. The pattern of variation with respect to time of the L norm of error is plotted for the following test problems:

P.P.1 $\quad -u_{xx}+\dot{u}=0 \qquad x \in \,]0,1[$

$u(o,t)=u(1,t)=0$

$u(x,o)=\sin \pi x$

Fig. 1 and 2 show the superior accuracy of the space-time elements at large time steps; they become comparable, accuracy-wise, with Galerkin method at small time steps.

P.P.2 $\quad -u_{xx}+\dot{u}=(\pi^2 t+1)\sin \pi x \qquad x \in \,]0,1[$

$u(0,t)=u(1,t)=0$

$u(x,0)=0$

The performance of space-time elements is overwhelming for a large range of time steps (Fig. 3,4)

P.P.3 $-k u_{xx}+\dot{u}=1$ $x \in]0,1[$

$u(0,t)=u(1,t)=0$

$u(x,0)=0$

For k=1, the space-time elements show instability at the end nodes, for large time steps (Fig. 5); with lower time step, and filtering the end nodes out of the computation of the error norm, the performance becomes comparable with Galerkin (Fig. 6). For k=0.2, the two methods perform comparably, with Galerkin on the upper side (Figs. 7,8). Further reduction of k to 0.1 brings the two methods even closer (Figs. 9,10).

Notice that the poor performance, in this test, of the space--time elements is to be attributed to the discontinuity at the boundary between forcing function and boundary conditions. The continuity forced in by the element shape function perturbs the nodes adjacent to the boundary, that undergo oscillations; these in turn can grow with time, affect other nodes and finally lead to instability.

P.P.4 $-u_{xx}+\dot{u}=2t-x(x-1)$ $x \in]0,1[$

$u(0,t)=1$

$u(1,t)=0$

$u(x,0)=1-x$

P.P.5 $-u_{xx}+\dot{u}=(\pi^2 t^2+2t)\sin \pi x$ $x \in]0,1[$

$u(0,t)=u(1,t)=0$

$u(x,0)=0$

In these problems with f(t), space-time elements overdo Galerkin at all time steps (Figs. 11 to 14)

5. WEAK FORMULATION FOR HYPERBOLIC PROBLEMS

Starting from a 2^{nd} order ellyptic operator as defined in par. [2], with the additional hypothesis that the operator be symmetric, i.e. that in eq. (1) $a_{ij}=a_{ji}$, and defining a family of cohercive and bounded bilinear forms as in egs (3) and (4), it can be proved [2] that: given $u_o \in H_o^1(\Omega)$, $u_1 \in L^2(\Omega)$, $f(x,t) \in L^2(C)$, there exists a unique fucntion $u(x,t) \in W(O,T)$ (1) such that

$$(19) \quad \int_0^T (a(t;u,v)-(\dot{u},\dot{v})_{L^2(\Omega)})dt = \int_0^T (f,v)_{L^2(\Omega)} dt + (u_1,v_0)_{L^2(\Omega)}$$

for every $v \in W(O,T)$ such that $v(T)=o$, and also

$$(20) \quad u(x,O)=u_o.$$

Equation (19) can be written in the form

$$(21) \quad \int_C (\sum_{i,j=0}^{n} a_{ij}(x,t) D_i u D_j v)\,dxdt - \int_C (\dot{u}.\dot{v})\,dxdt =$$
$$\int_C (f.v)\,dxdt + (u_1,v_O)_{L^2(\Omega)}$$

Equation (21) represents the weak formulation for a linear hyperbolic problem, as it can be proved [2] that:

a) $< Au+\ddot{u}, v > = (f,v)_{L^2(C)} \quad , v \in C_0^\infty(C)$

therefore

$$Au+\ddot{u}=f$$

in the sense of the distributions on C;

---

(1) We call W(o,T) the space of real functions v(x,t) defined on C, such that $v \in L^2(O,T;H_o^1(\Omega)), \dot{v} \in L^2(C)$

b) $\lim_{t \to o} (\dot{u},v)_{L^2(\Omega)} = (u_1,v)_{L^2(\Omega)} \quad ,v \in L^2(\Omega)$

therefore $\dot{u}$ tends, for t going to O, to u_1 weakly in $L^2(\Omega)$;

c) $u(x,t)=o$ for every $(x,t) \in \partial\Omega \times I$

as $u(x,t) \in L^2(o,T;H_o^1(\Omega))$

6. SPACE-TIME APPROXIMATION (HYPERBOLIC)

For sake of simplicity we make reference to the following one-dimensional problem, that prototypes the wave propagation in a rod (zero damping)

Problem PI

(22.1) $\quad -Ku_{xx}+\rho\ddot{u}=f(x,t) \qquad x \in]O,b[, \quad t \in]o,T[$

(22.2) $\quad u(x,o)=u_o$

(22.3) $\quad \dot{u}(x,o)=\dot{u}_o$

(22.4) $\quad u(o,t)=u(b,t)=o$

the weak formulation (21) applied to problem (22) gives

(23) $\quad k((u_x,v_x))-\varrho((\dot{u},\dot{v}))=((f,v))+\rho((\dot{u}_o,v_o))$

Partitioning the domain $[o,b] \times [o,T]$ into space-time elements $[o,a] \times [o,\tau]$, and using a bilinear approximating function inside the element (see par. 3) one obtains for the assembled equations.

(24) $\quad \underline{u}K_x\underline{v}-\underline{u}K_{tt}\underline{v}=\underline{f}F\underline{v}+\underline{\dot{u}}_oP\underline{v}_o$

where the matrices K_x, K_{tt}, F, P are given in Appendix 1 Calling $M=K_x-K_{tt}$, partitioning eqs (24) into two blocks, at time $t=o$ and $t=\tau$, as in par. 3 and introducing conditions (14) and (15) one obtains

(25) $\underline{u}_1 M_{11} \underline{v}_1 + \underline{u}_2 M_{21} \underline{v}_1 = \underline{f} F_1 v_1 + \dot{\underline{u}}_1 P \underline{v}_1$

eliminating $\underline{v}_1$, carrying the term with $\underline{u}_1$ on the right end side and transposing the equations, one finally obtains

(26) $M_{21}^T \; \underline{u}_2 = F_1^T \underline{f} + P_1^T \dot{\underline{u}}_1 - M_{11}^T \underline{u}_1$

Solving eq (26) in $\underline{u}_2$ provides the required nodal values of the unknown function u at the time t=T. The same considerations a,b,c made in par. 3 for parabolic problems apply here for the hyperbolic ones. The only difference is that here $\dot{\underline{u}}_1$, the vector of nodal velocities is given only at t=o; at the subsequent time steps $\dot{\underline{u}}_1$ must be approximated, as the procedure produces only the nodal displacements $\underline{u}_1$ at each step.

After testing several techniques for approximating $\dot{\underline{u}}_1$, it was found that computing $\hat{\underline{u}}_2$ at a time step close to τ:

(27) $\hat{t} = \psi\tau \;, \; 0 < \psi < 2 \quad , \quad \psi \neq 1$

and approximating the time derivative with the incremental ratio

(28) $\dot{\underline{u}}_1 \simeq (\underline{u}_2 - \hat{\underline{u}}_2) / \, |\, \tau - \psi\tau |$

may lead to unexpected accuracy of integration. Notice that in eq (28) the terms on the right end side belong to, say, step n of integration, while $\dot{\underline{u}}_1$ is refered to step n+1.

The peak of accuracy occurs when the "optimal" value ψ_o of ψ is used. This can be easily computed:

1.- the wave equations are integrated throughout a half wavelength using an initial value ψ_1 of ψ, and the error e_1 in the displacement (it should be zero; the computed value coincides with the error) is recorded;

2. - the step is repeated with another trial value ψ'_2; e_2 is recorded;

3. - the optimal value ψ_o is derived from linear extrapolation on the two previously computed points:

$$\psi_o = \psi_1 + e_1 \frac{\psi_2 - \psi_1}{e_2 - e_1} \tag{29}$$

Several numerical tests on problem PI have shown that the relationship between e and ψ is indeed linear (see figs. 15,16,17); therefore linear extrapolation is justified.

The accuracy obtained with ψ'_o, in the test problem, has been superior to the accuracy obtained introducing into eq (26) the exact value $\dot{u}_1$ of the velocity.

In fig. 18 the values of the error e for the integration of problem PI across the first wave-length are displayed against different values of mesh size, time step and ψ.

7. NUMERICAL TESTS (HYPERBOLIC)

A set of one-dimensional wave propagation problems (zero damping) was selected to test the numerical accuracy of space-time elements againts Newmark's method (see [9]) (γ=1/2, β=o; it coincides with central differences, that have shown [8] to be the most accurate Galerkin-type operator for the undamped wave problems).

The comparison is made with the same, fix, space discretization and with the same, variable, time step; the latter is tuned to the problem, in order to fall below the stability limit. Here, as for parabolic test problems, the exact solution is known, the error is computed at all time steps and displayed.

P.I. 1 $-u_{xx}+\ddot{u}=o$ $x\in]o,\pi[$

$u(o,t)=u(\pi,t)=o$

$u(x,o)=o$

$\dot{u}(x,o)=\sin x$

the displacement of the mid point is shown for different space discretizations(α=1/2,1/4 : no.of partitions nodes in the domain) and for different time steps, against the exact solution (solid line). In fig. 19, with the coarse mesh and step, space-time elements perform quite well, while Galerkin is soon out of phase; improving the time step doesnt help Galerkin (fig.23). Improving the mesh (fig. 20,21) leads the space-time elements to negligible errors and Galerkin to a reasonable performance.

P.I. 2 $-u_{xx}+\ddot{u}=\pi^2 t\sin(\pi x)$ $x\in]o,1[$

$u(o,t)=u(1,t)=o$

$u(x,o)=o$

$\dot{u}(x,o)=\sin\pi x$

In such a problem with f(t) the amplitude of the wave grows linearly with respect to time. The displacement of the midpoint is shown as a function of time in figs 23 and 24. Space-time elements perform quite well, while Galerkin shows a loss of accuracy in time almost insensible to the time step.

P.I. 3 $-u_{xx}+\ddot{u}=(2+t^2\pi^2)\sin(\pi x)$ $x\in]o,1[$

same initial and boundary conditions as in P.I.2 Here the amplitude of the wave grows quadratically with respect to time. The same relative considerations as for the previous test apply (see figs 25 and 26).

8. CONCLUSIONS

The discretization of the variational theory for parabolic and hyperbolic operators developed by Lions and Magenes [2] has proved to produce, at the same computational costs, an outstanding numerical accuracy, compared with the optimal Galerkin methods. The authors propose the following explanation: introducing into the discretized equations both the initial conditions on the unknown function u and the "final" conditions (v(T)=o) on the test function v, leads to solving a linear set of equations in $\underline{u}_2=\underline{u}(T)$ with the matrix K_{12}, i.e. the off-diagonal matrix of the space-time elements i.e. the matrix connecting the values of u at t=o an at t=T namely the evolution matrix. Galerkin methods on the other hand solve with K_{11}, namely with the distribution matrix. Whenever a physical phenomenon evolves rapidly, space-time elements should pick it up better. The oustanding accuracy for time-dependent problems prove it.

REFERENCES

1. S. Agmon, Lectures on Elliptic Boundary Problems, Van Nostrand Mathematical Studies, (1965).
2. J. L. Lions, E. Magenes, Non Homogeneous Boundary Value Problems and Applications, Vols I, II, III, Springer (1972).
3. M. Morandi Cecchi, A. Cella, An Extended Theory of Finite Elements, in C. A. Brebbia, H. Tottenham: (eds) Variational Methods in Engineering, Southampton University Press (1974).
4. M. Morandi Cecchi, A. Cella, A. Ritz - Galerkin approach to heat conduction: method and results, Proceedings 4th CANCAM Conf., Ecole Polytechnique, Montreal, (1973), session H, 767-768.
5. J. C. Bruch, G. Zyvoloski, Transient two-dimensional heat conduction problems solved by the finite element method, Int. J. Num. Meth. in Eng., 8, (1974), 481-494.
6. O. C. Zienkiewicz, C. J. Pareh, Transient field problems: two dimensional and three dimensional analysis by isoparametric finite elements, Int. J. Num. Meth. in Eng., 2, (1970), 61-71.
7. M. Zlamal, Finite element methods in heat conduction problems, in J. R. Whiteman (ed) The Mathematics of Finite Elements and Applications II, Academic Press, London (1975), 85-104
8. A. Cella, On the accuracy and stability of the finite element approximation for parabolic and hyperbolic operators, in J. R. Whiteman (ed) The Mathematics of Finite Elements and Applications II, Academic Press, London (1975), 183-190.
9. G. L. Goudreau, R. L. Taylor, Evaluation of numerical integration methods in elastodynamics, Comp. Meth. Mech. Eng., 2 (1973), 69-97.
10. A. Cella, M. Lucchesi, Space-time elements for the wave propagation problem, Meccanica 10, (1975), 168-170.
11. M. Morandi Cecchi, Error estimates for finite elements solution of heat transfer problems in the space-time domain, in J. R. Whiteman (ed) The Mathematics of Finite Elements and Applications II, Academic Press, London (1975), 201-207.
12. J. J. Oden, Finite Elements of Nonlinear Continua, McGraw Hill (1971).

APPENDIX 1

Development of space-time stiffness matrices.

$u \simeq \underline{p}\underline{\alpha} = (1, x, t, xt)\{\alpha_1, \alpha_2, \alpha_3, \alpha_4\}$

$\underline{\alpha} = N\underline{u} \quad u \simeq \underline{p}N\underline{u}$

$$N = \begin{bmatrix} 1 & 0 & 0 & 0 \\ -1/a & 1/a & 0 & 0 \\ -1/\tau & 0 & 1/\tau & 0 \\ 1/a\tau & -1/a\tau & -1/a\tau & 1/a\tau \end{bmatrix}$$

$u_x \simeq \tilde{\underline{p}}\underline{\alpha} = \tilde{\underline{p}}\, N\underline{u}; \quad \tilde{\underline{p}} = (0, 1, 0, t)$

$u_t \simeq \hat{\underline{p}}\underline{\alpha} = \hat{\underline{p}}N\underline{u} \; ; \quad \hat{\underline{p}} = (0, 0, 1, x)$

$$k((u_x, v_x)) = k \int_0^\tau \int_0^a \underline{u}N\tilde{p}\tilde{p}N\underline{v}\, dxdt$$

$$= \underline{u}K_x\underline{v}; \quad K_x = \frac{k}{3}\frac{\tau}{a}\begin{bmatrix} A & \frac{1}{2}A \\ \frac{1}{2}A & A \end{bmatrix} \; ; \quad A = \begin{bmatrix} 1 & -1 \\ -1 & 1 \end{bmatrix}$$

$$c((u, \dot{v})) = c \int_0^\tau \int_0^a \underline{u}Np\hat{p}N\underline{v}\, dxdt$$

$$= \underline{u}K_t\underline{v}; \quad K_t = c\,\frac{a}{6}\begin{bmatrix} -B & B \\ -B & B \end{bmatrix}; \quad B = \begin{bmatrix} 1 & \frac{1}{2} \\ \frac{1}{2} & 1 \end{bmatrix}$$

$\underline{f} \simeq \; \alpha = \underline{p}\; N\; \underline{f}$

$((f, v)) = \underline{f}F\underline{v} \qquad F = \frac{a\tau}{9}\begin{bmatrix} B & \frac{1}{2}B \\ \frac{1}{2}B & B \end{bmatrix}$

$u_o \simeq \underline{p}^0 N\underline{u}_o \qquad \underline{p}^0 = (1, x, 0, 0)$

$(u_o, v_o) = u_o Q v_o; \qquad Q = \frac{a}{3}\; cB$

$$\varrho((\dot{u},\dot{v}))= \varrho\int_0^T \int_0^a \underline{u}N\overset{\checkmark\checkmark}{pp}Nv\ dxdt$$

$$=\underline{u}\ K_{tt}\ \underline{v}; \qquad K_{tt}=\frac{1}{3}\frac{\varrho a}{\tau}\begin{bmatrix} B & -B \\ -B & B \end{bmatrix}$$

$$\varrho\ (\dot{u}_o, v_o) = \underline{\dot{u}}_o P \underline{v}_o; \qquad P= \frac{a}{3}\ \rho\, B B$$

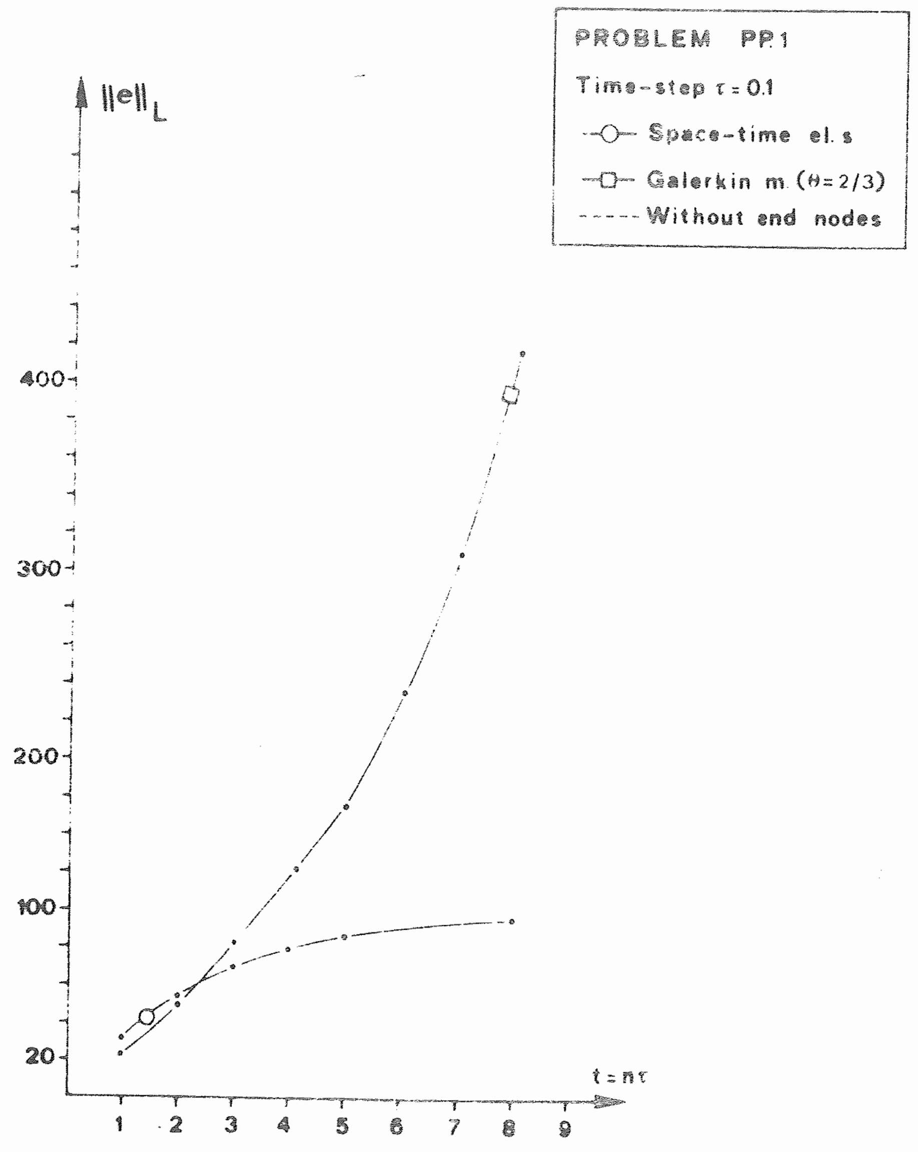

Fig. 1 - Test on linear parabolic.

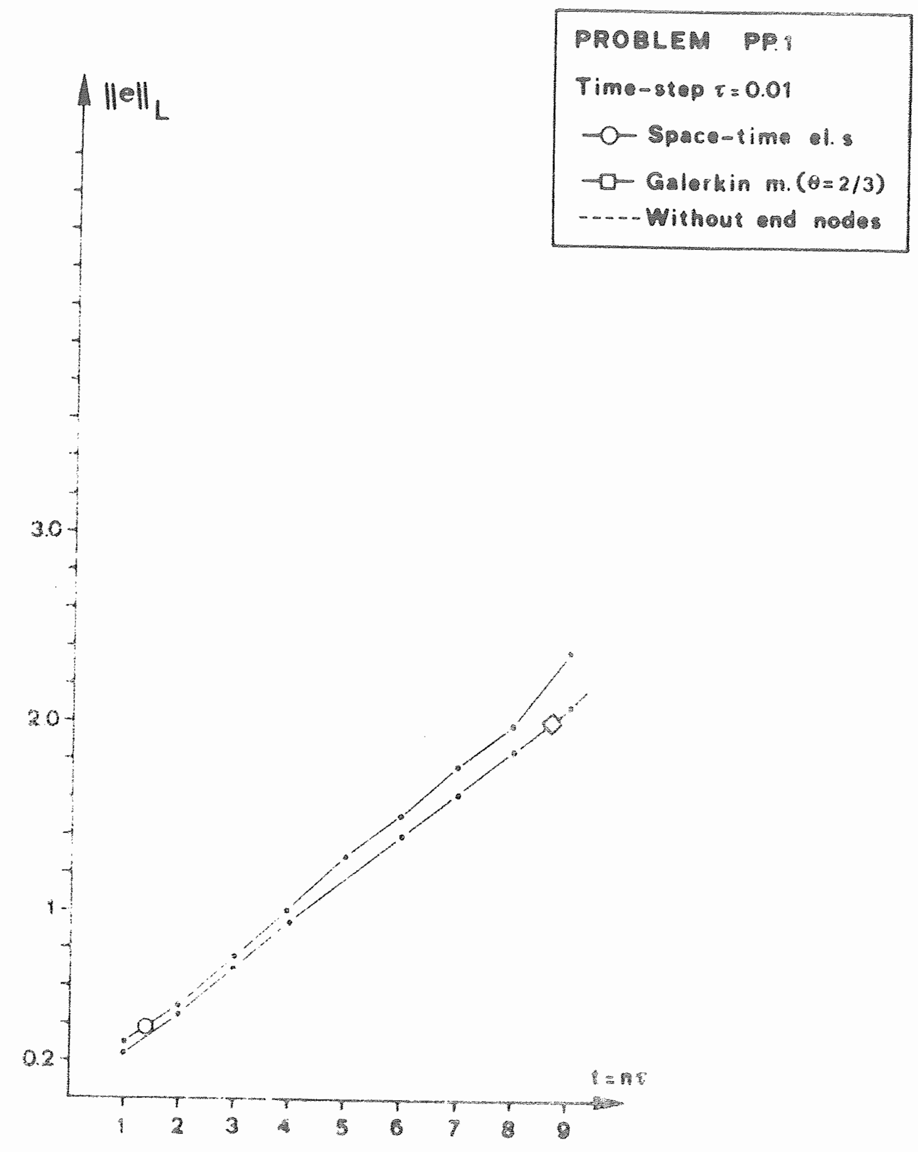

Fig. 2 - Test on linear parabolic.

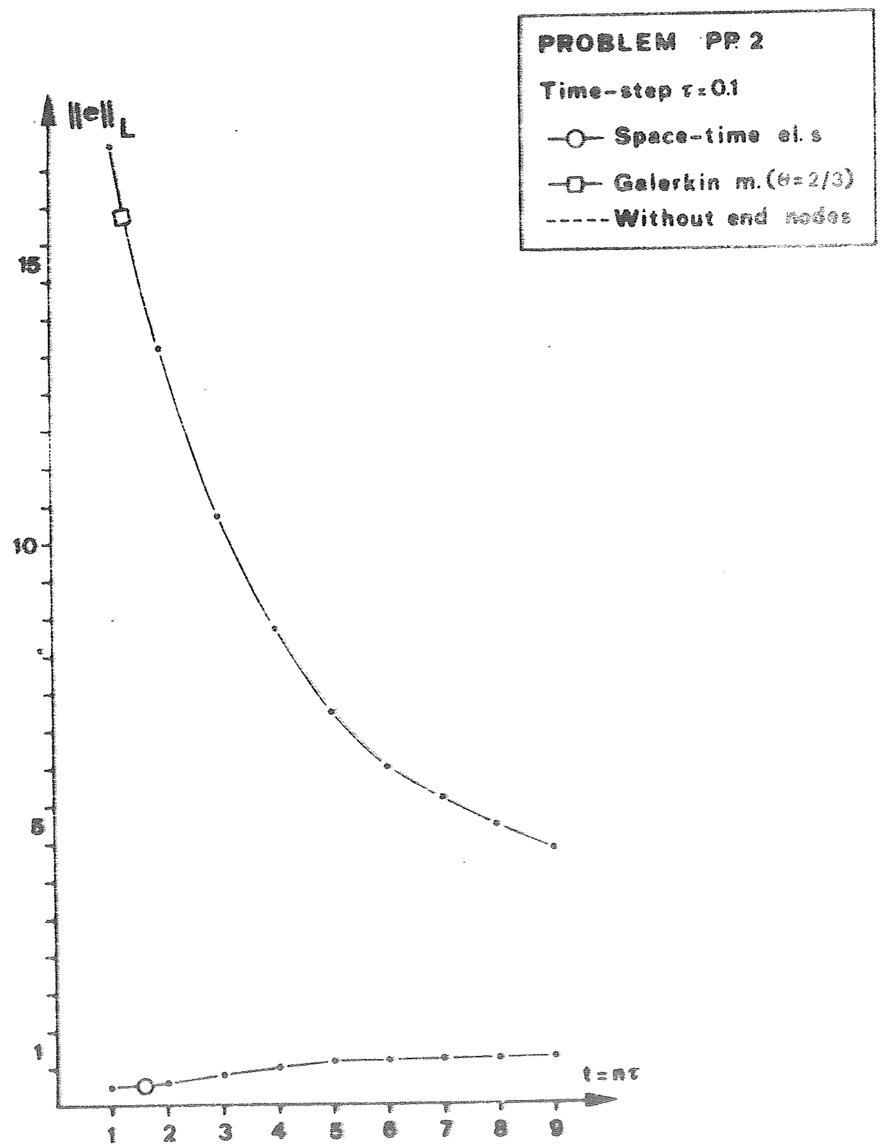

Fig. 3 - Test on linear parabolic.

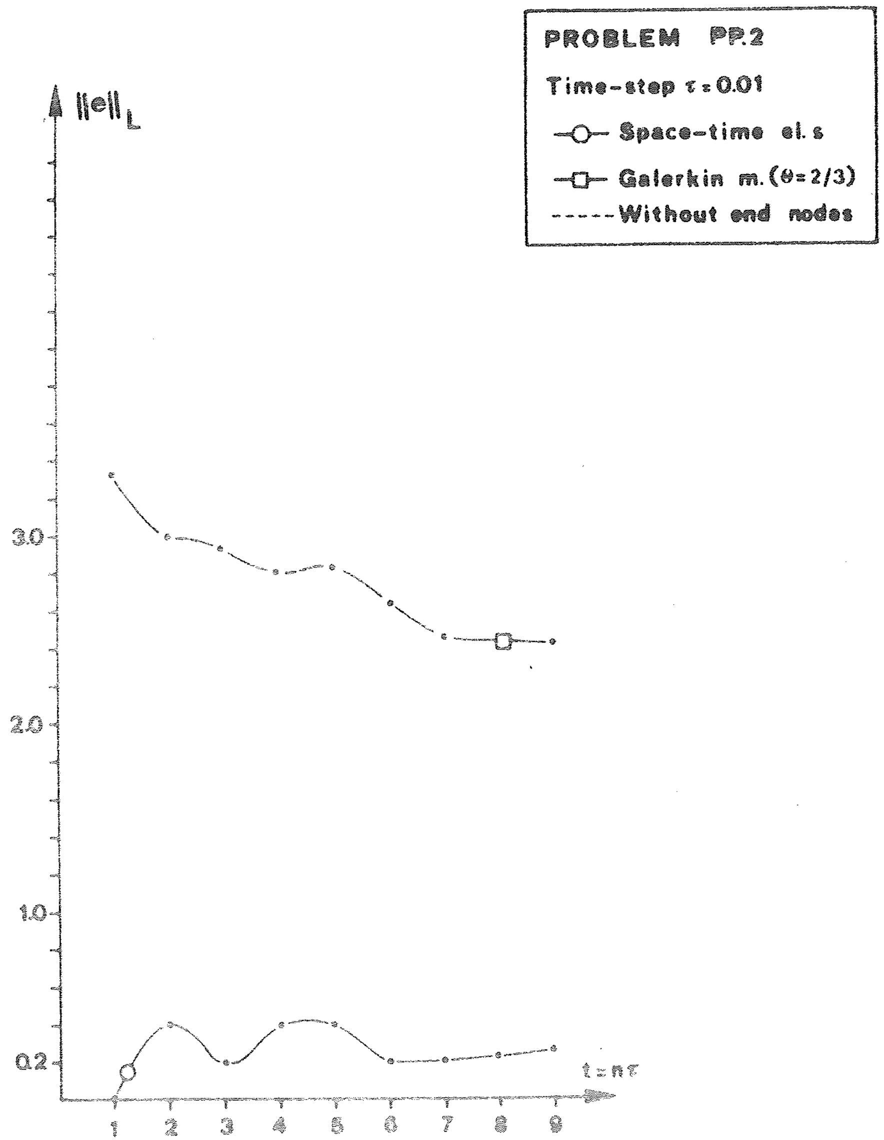

Fig. 4 - Test on linear parabolic.

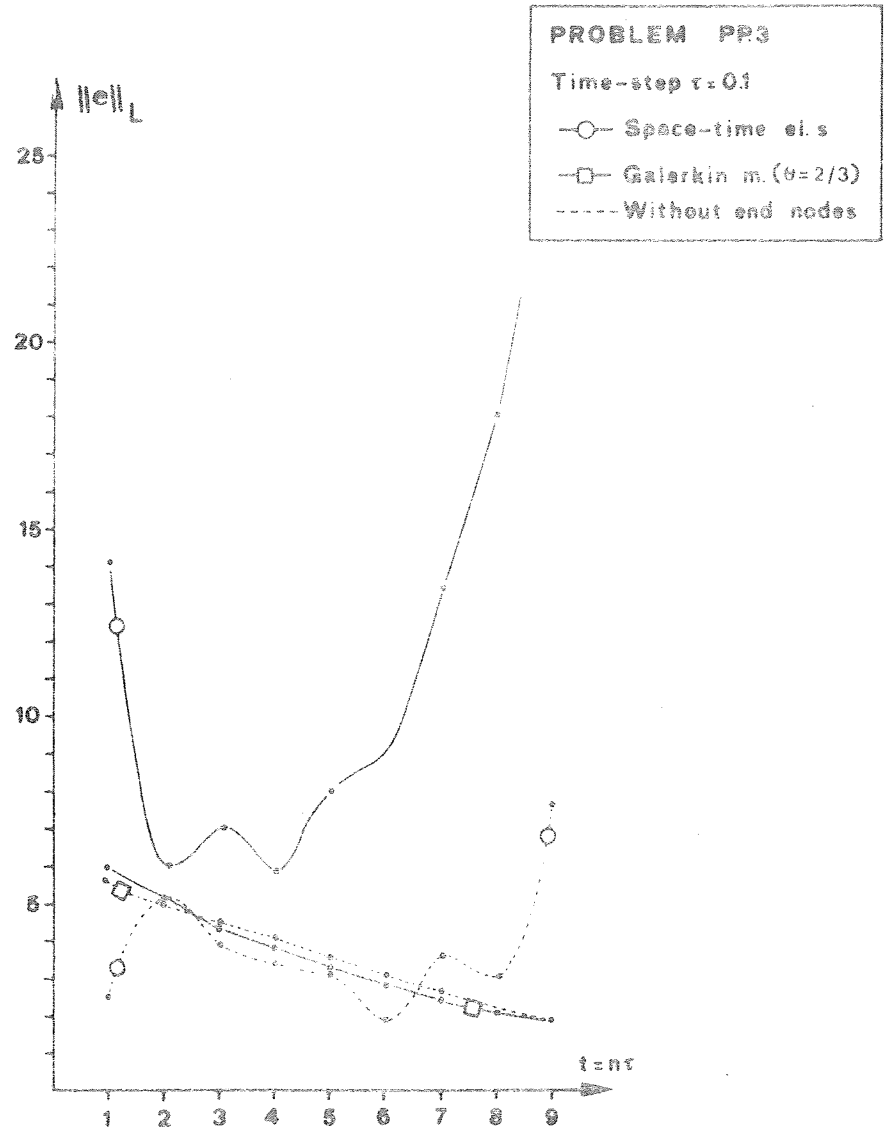

Fig. 5 - Test on linear parabolic (K=1).

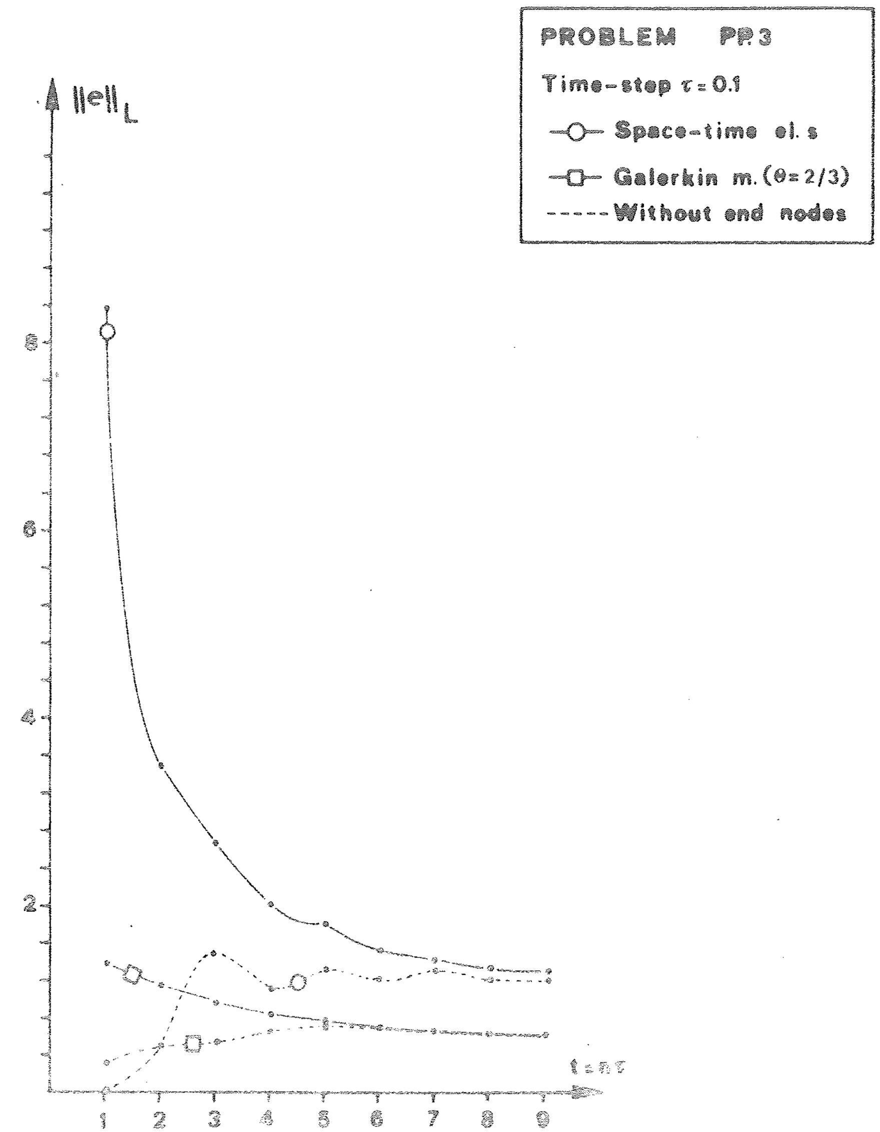

Fig. 6 - Test on linear parabolic (K=1).

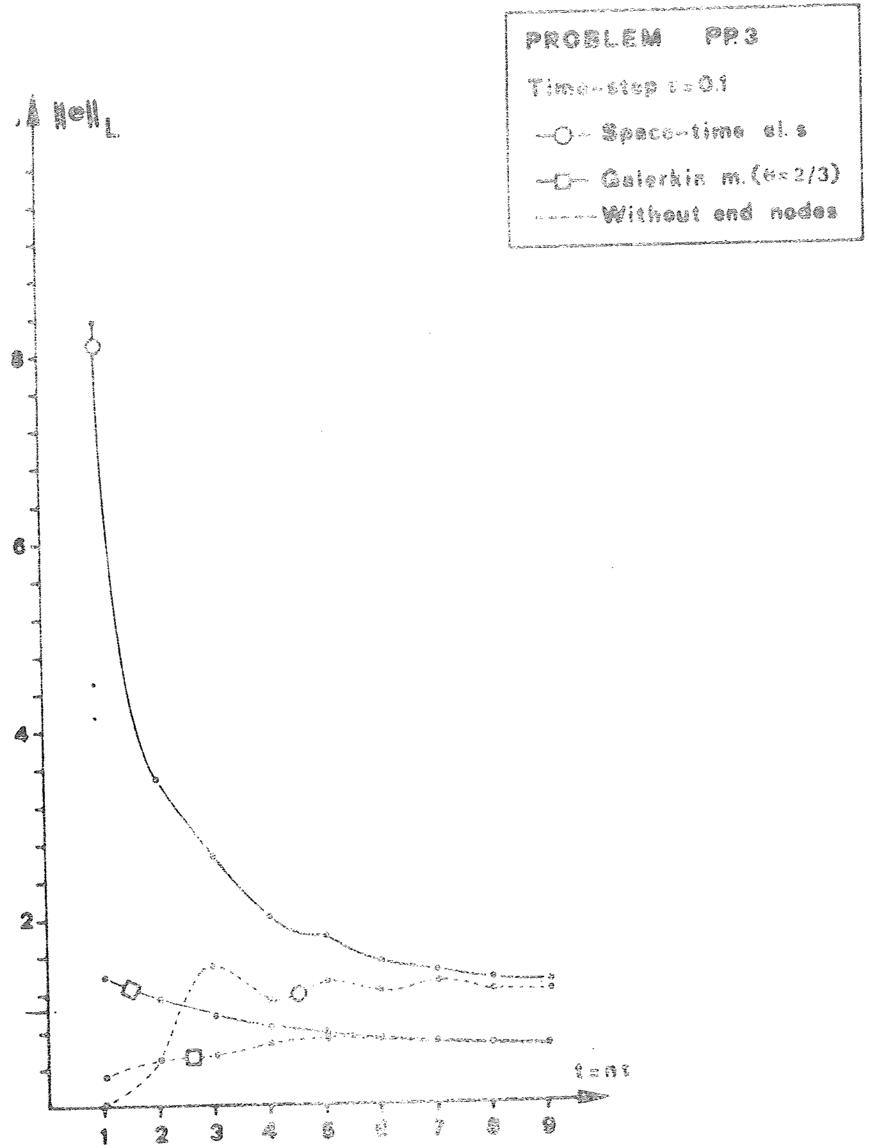

Fig. 7 - Test on linear parabolic (K=0.2).

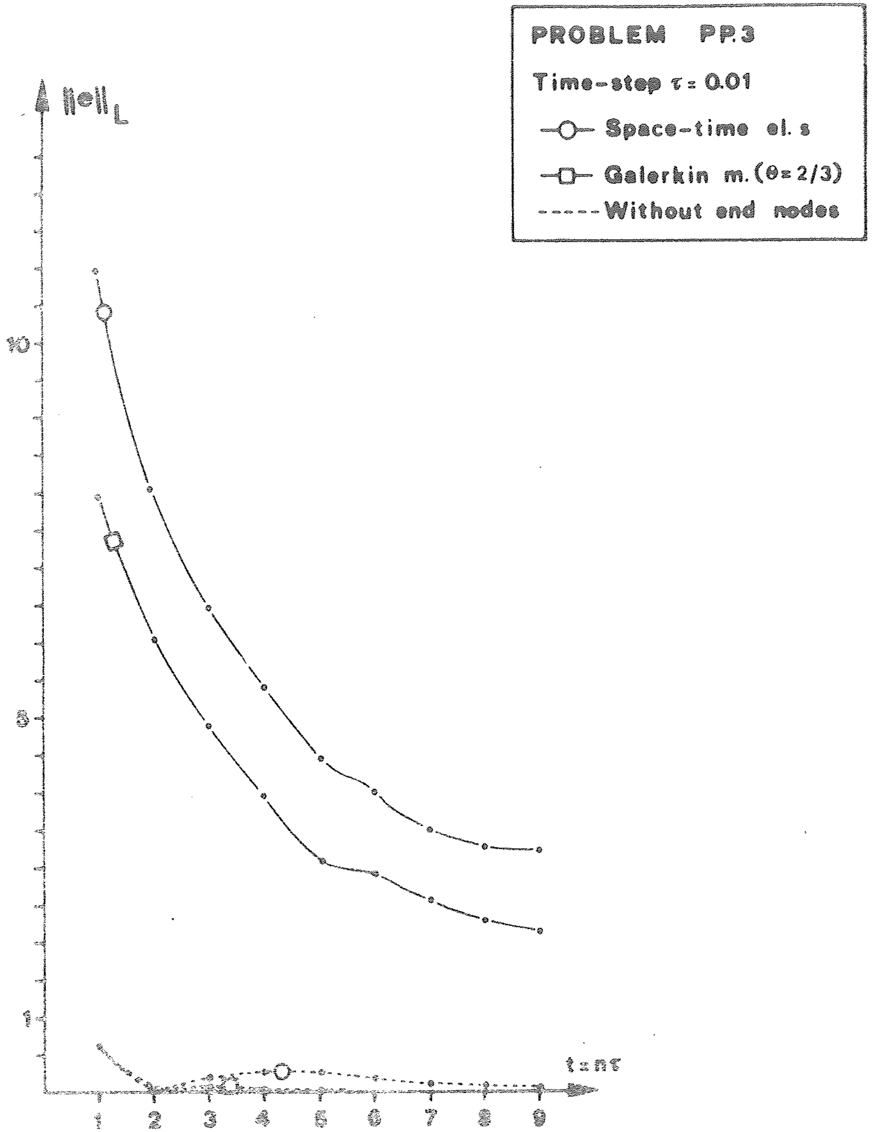

Fig. 8 - Test on linear parabolic (K=0.2).

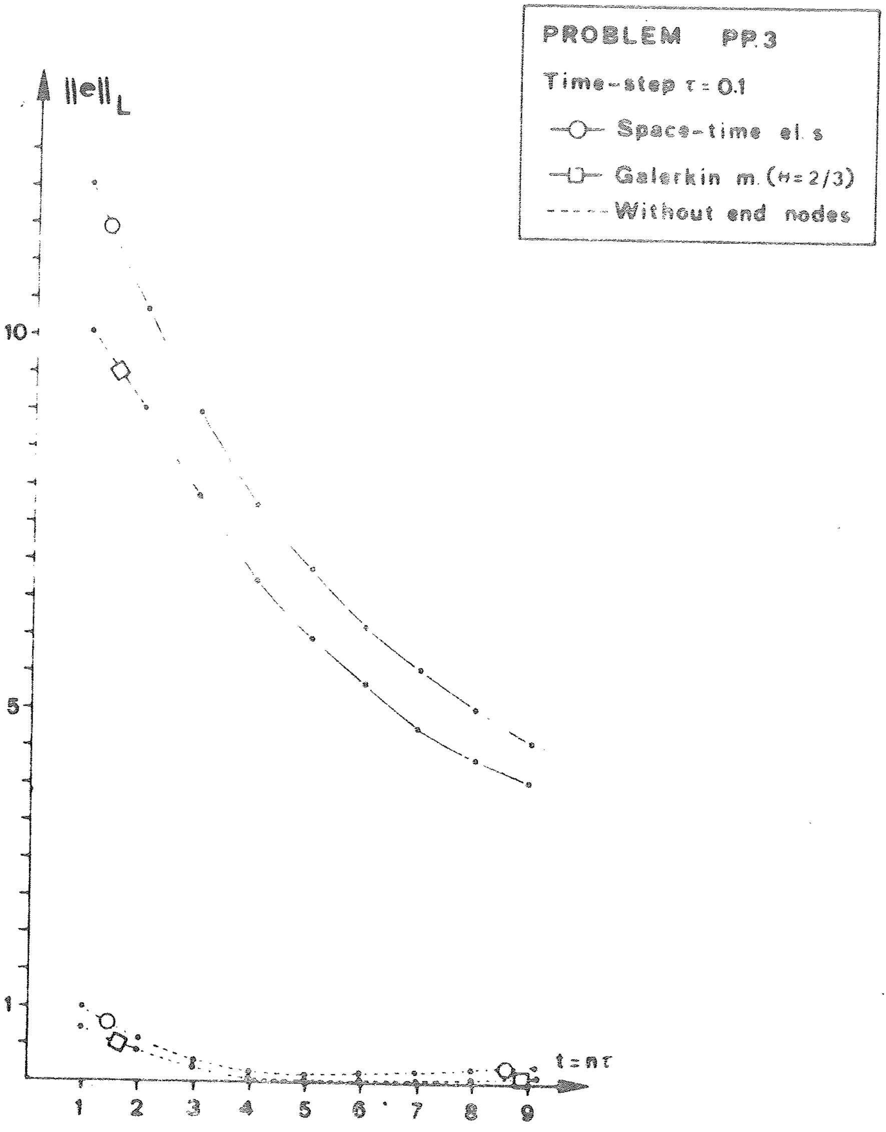

Fig. 9 - Test on linear parabolic (K=0.1).

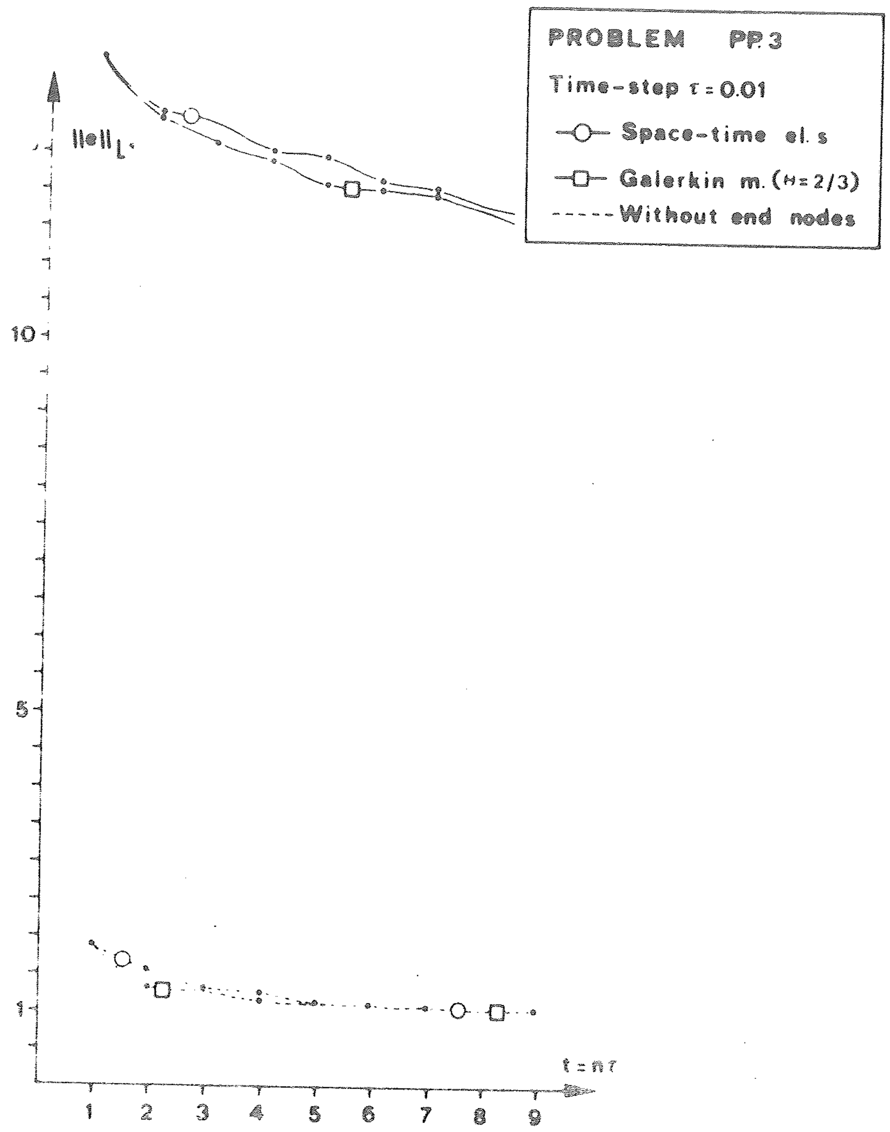

Fig. 10 - Test on linear parabolic (K=0.1).

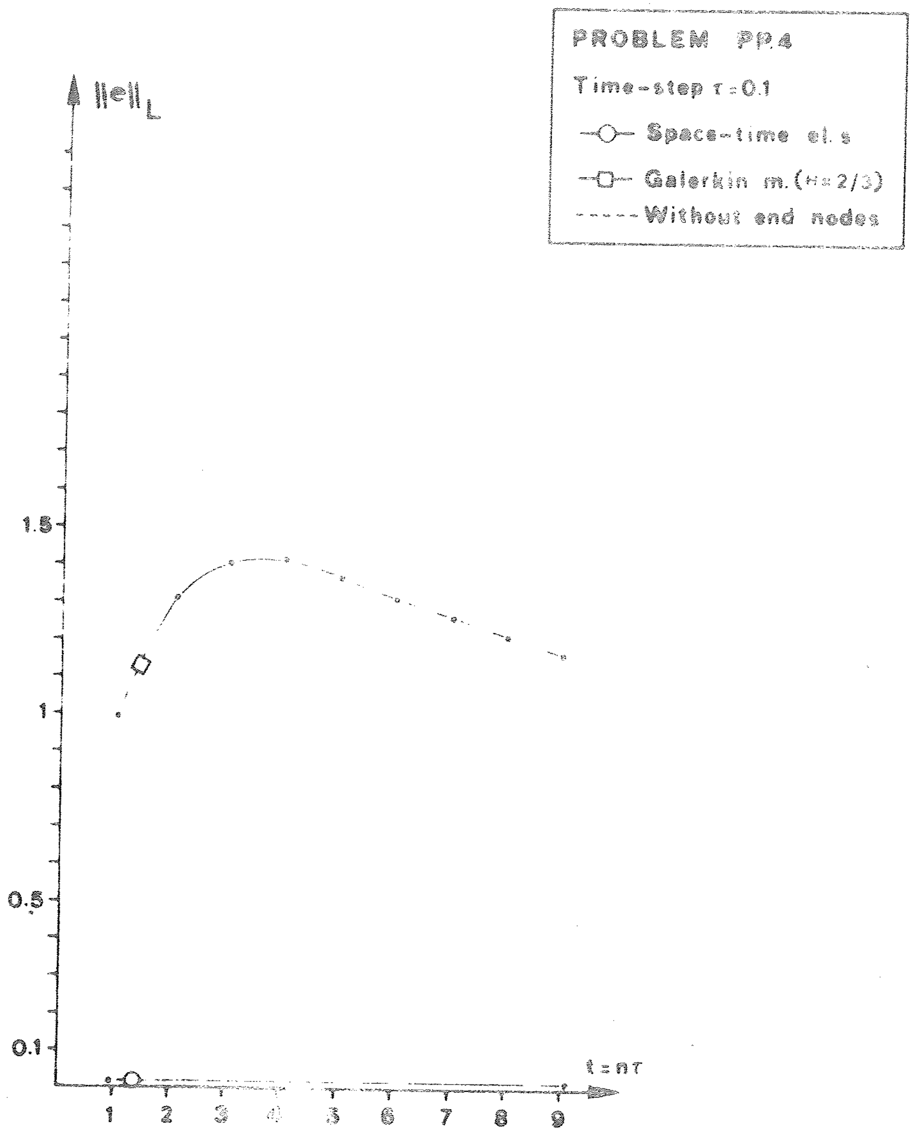

Fig. 11 - Test on parabolic with f(t)

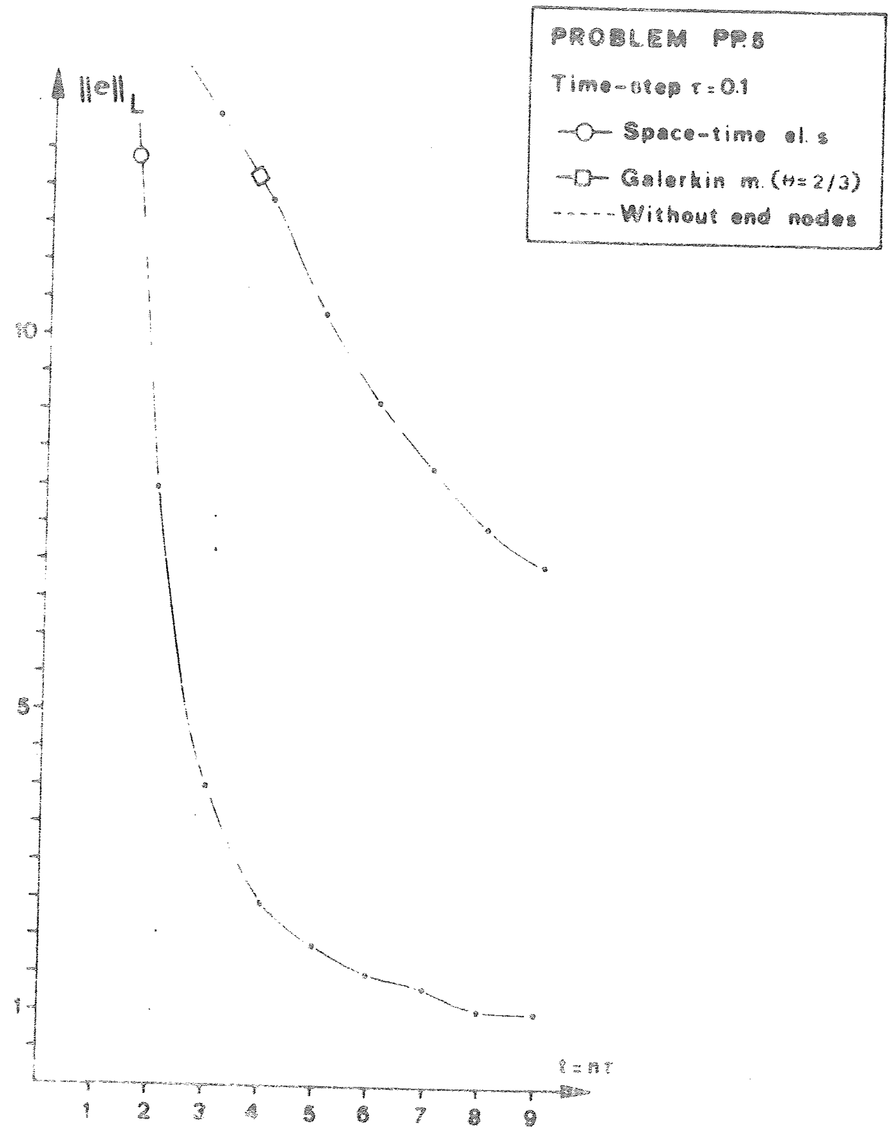

Fig. 12 - Test on parabolic with f(t)

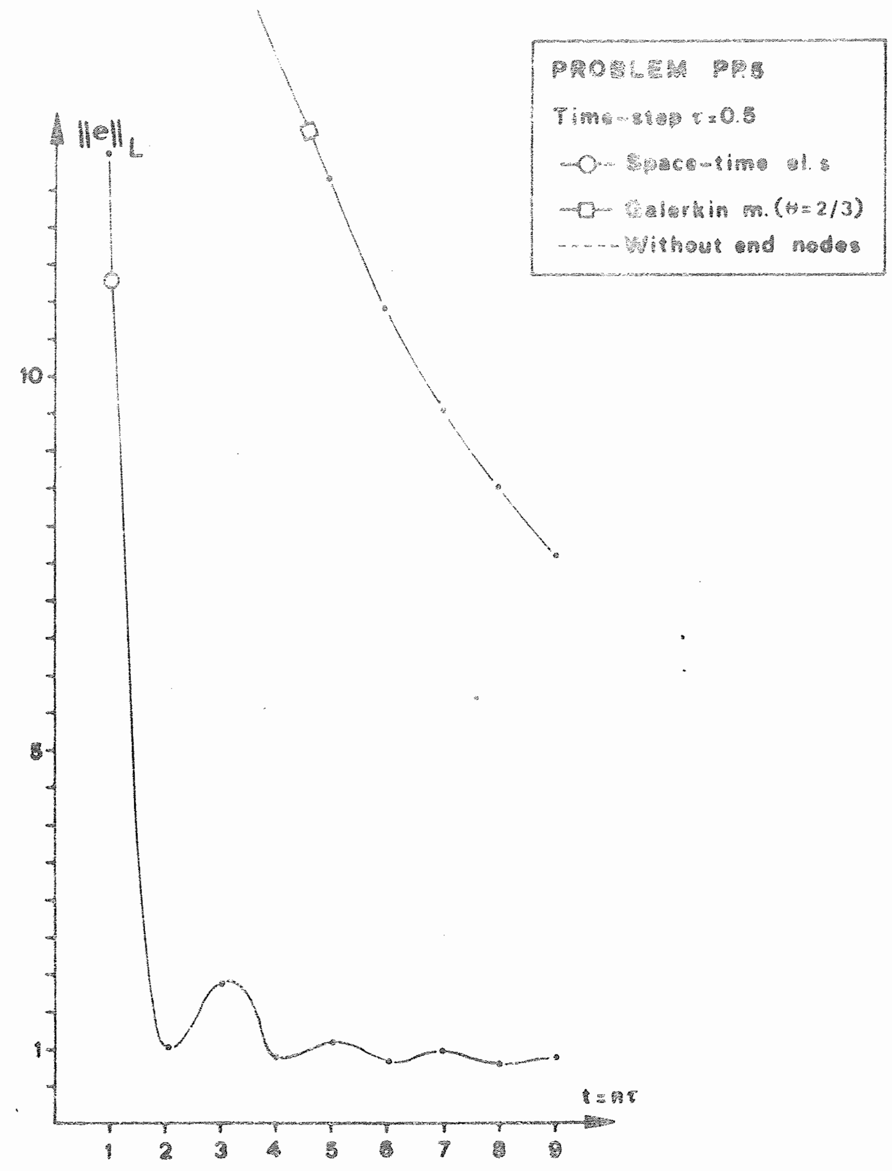

Fig. 13 - Test on parabolic with f(t)

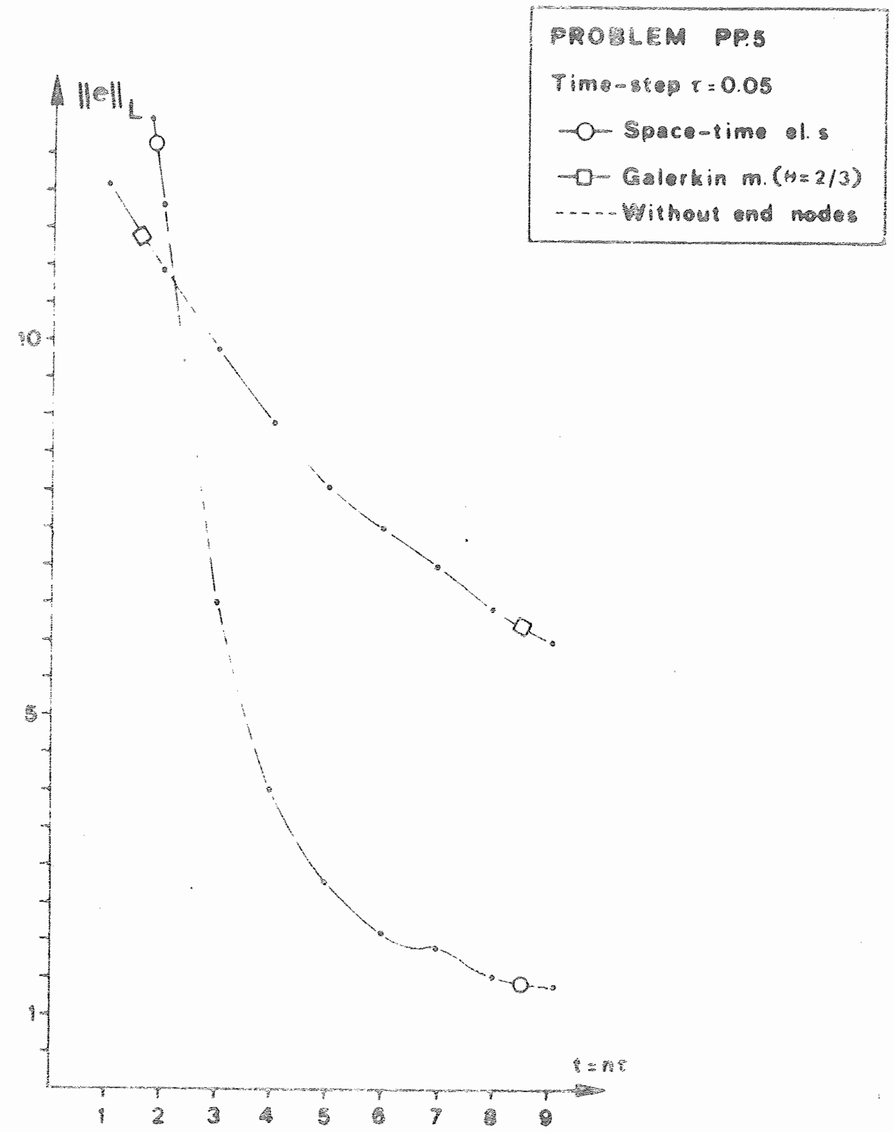

Fig. 14 - Test on parabolic with f(t)

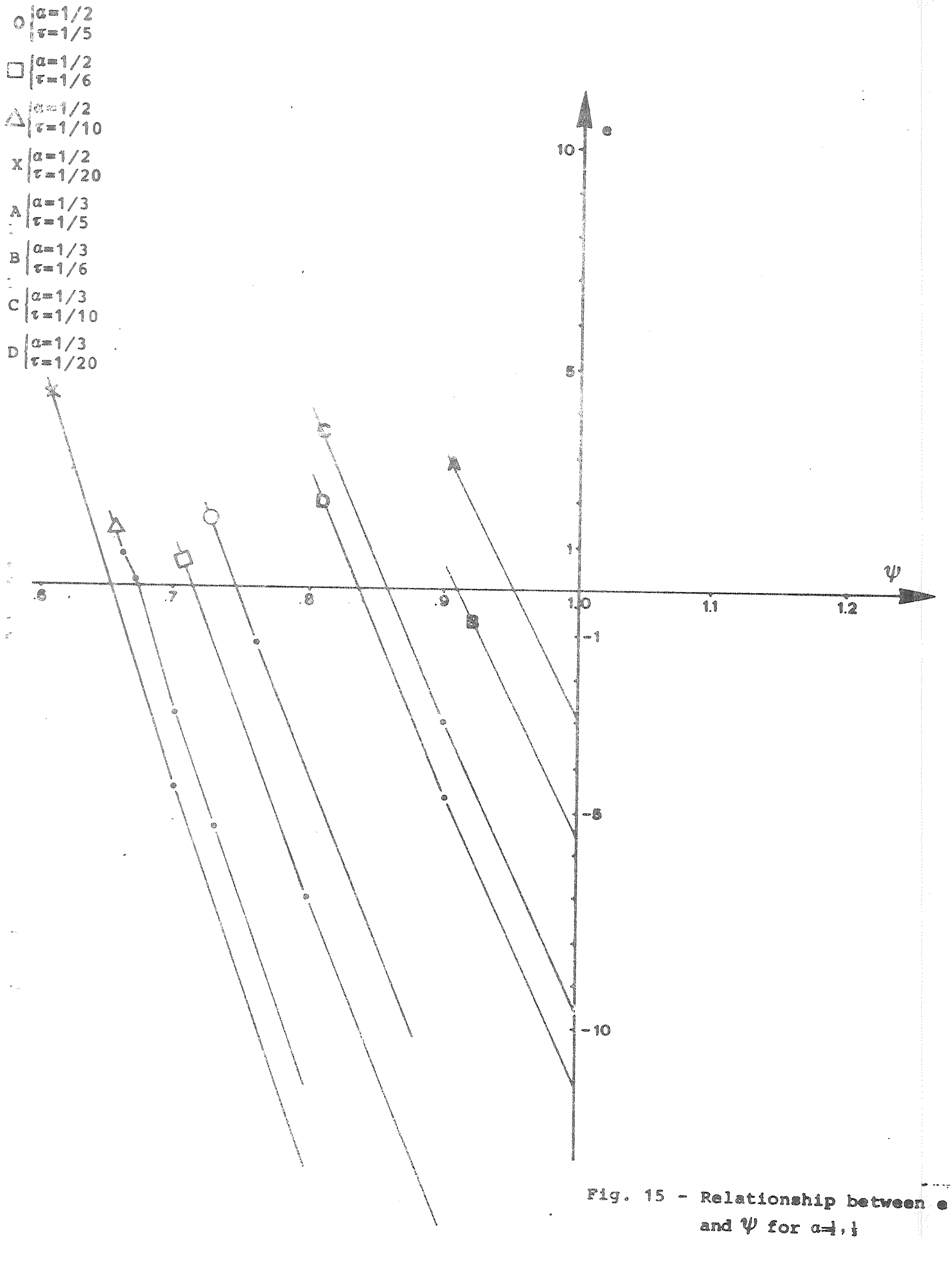

Fig. 15 - Relationship between e and ψ for $\alpha = \frac{1}{2}, \frac{1}{3}$

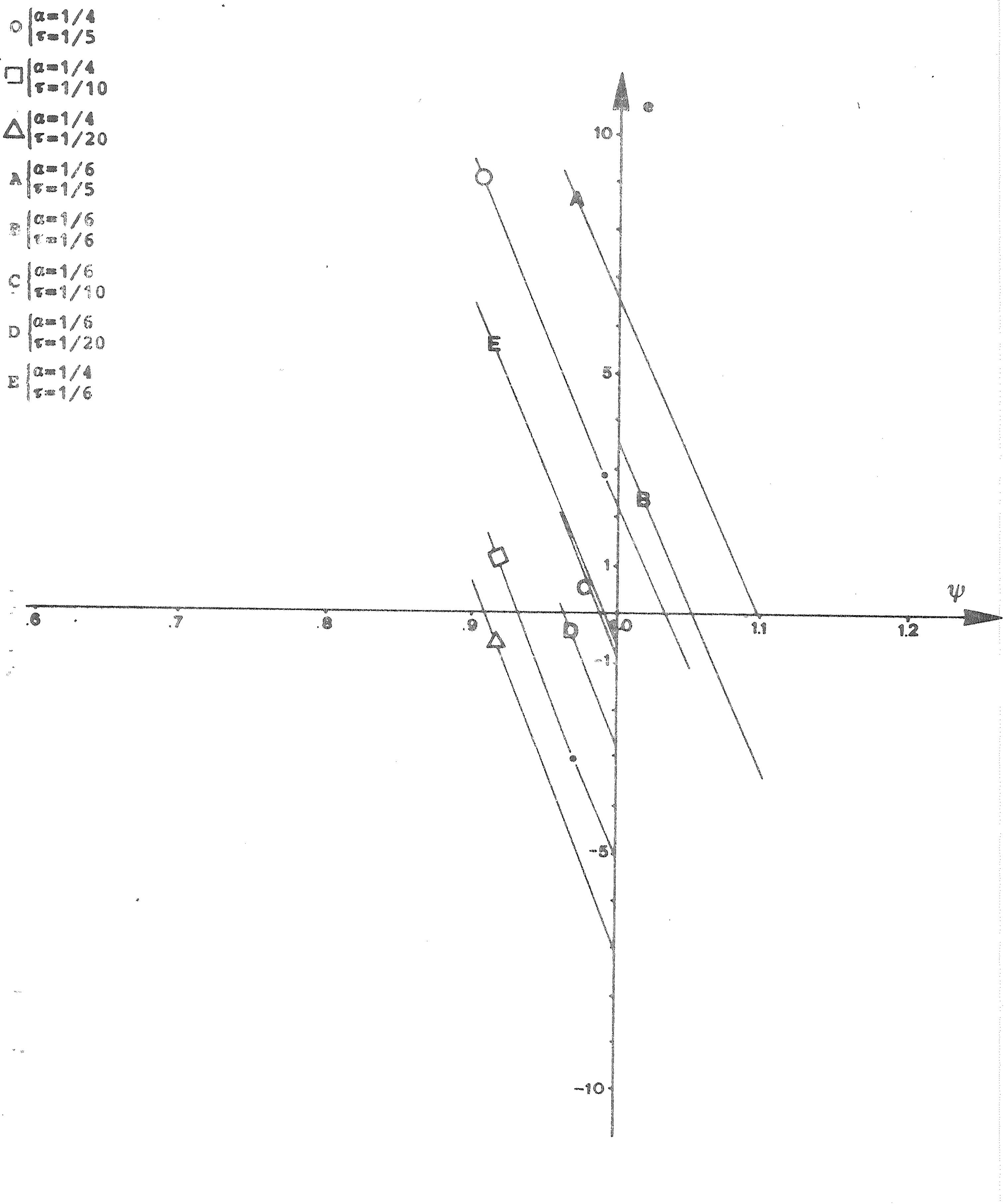

Fig. 16 - Relationship between e and ψ for $\alpha = \frac{1}{4}, \frac{1}{6}$

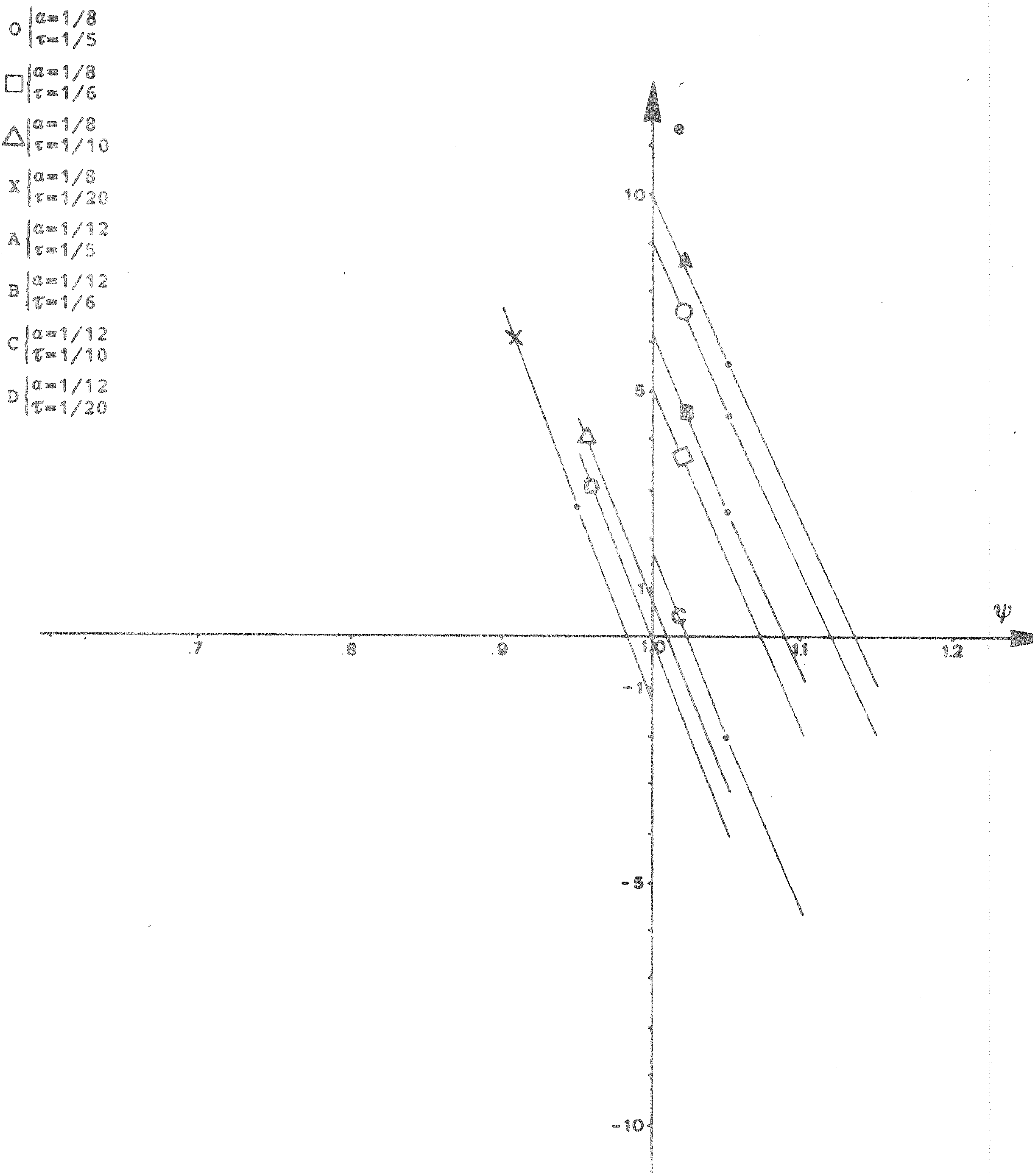

Fig. 17 - Relationship between e and ψ for $\alpha = \frac{1}{8}, \frac{1}{12}$

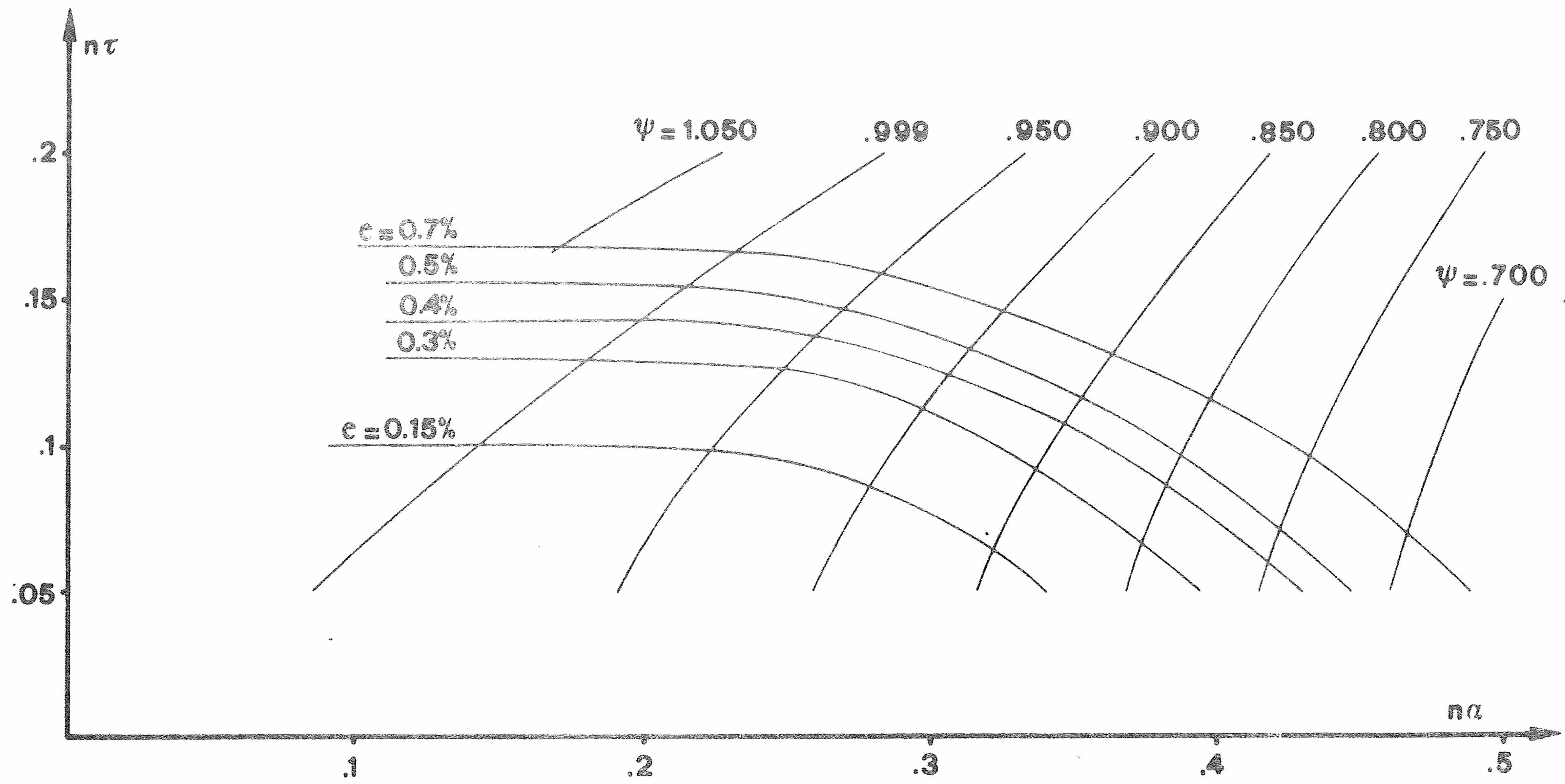

Fig. 18 - Chart of the error e againts different values of α, τ, ψ

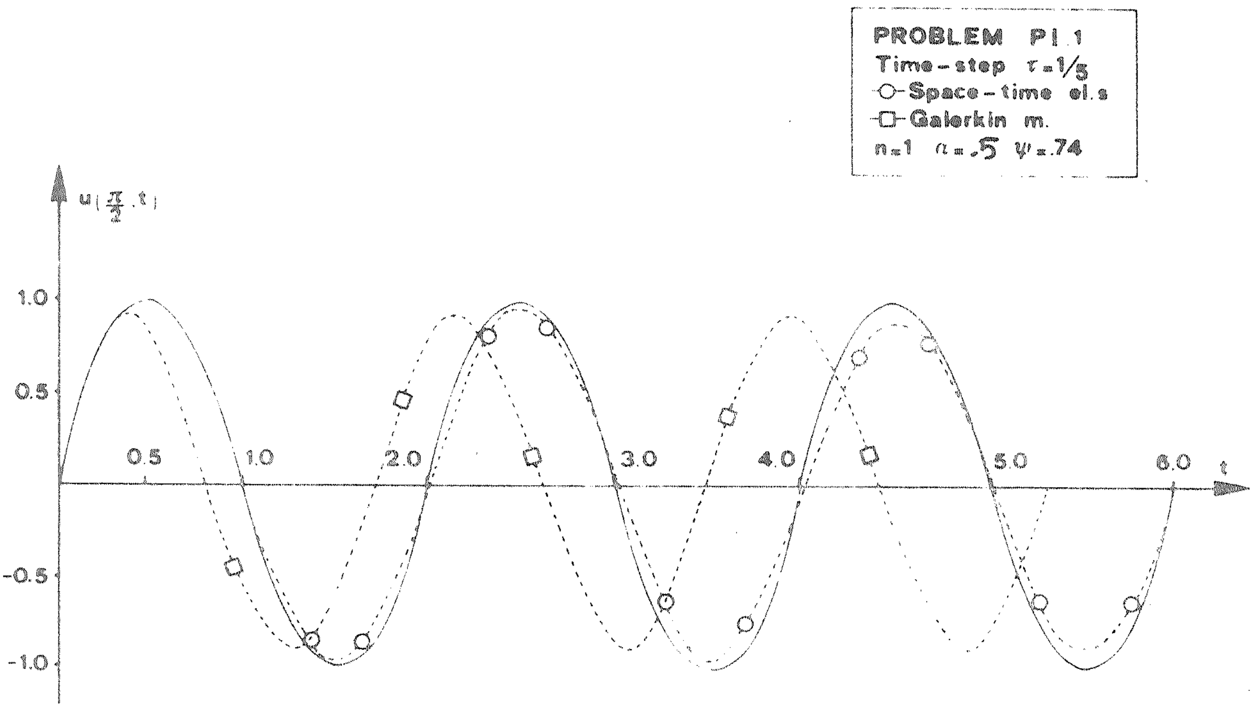

Fig. 19 - Test on linear hyperbolic.

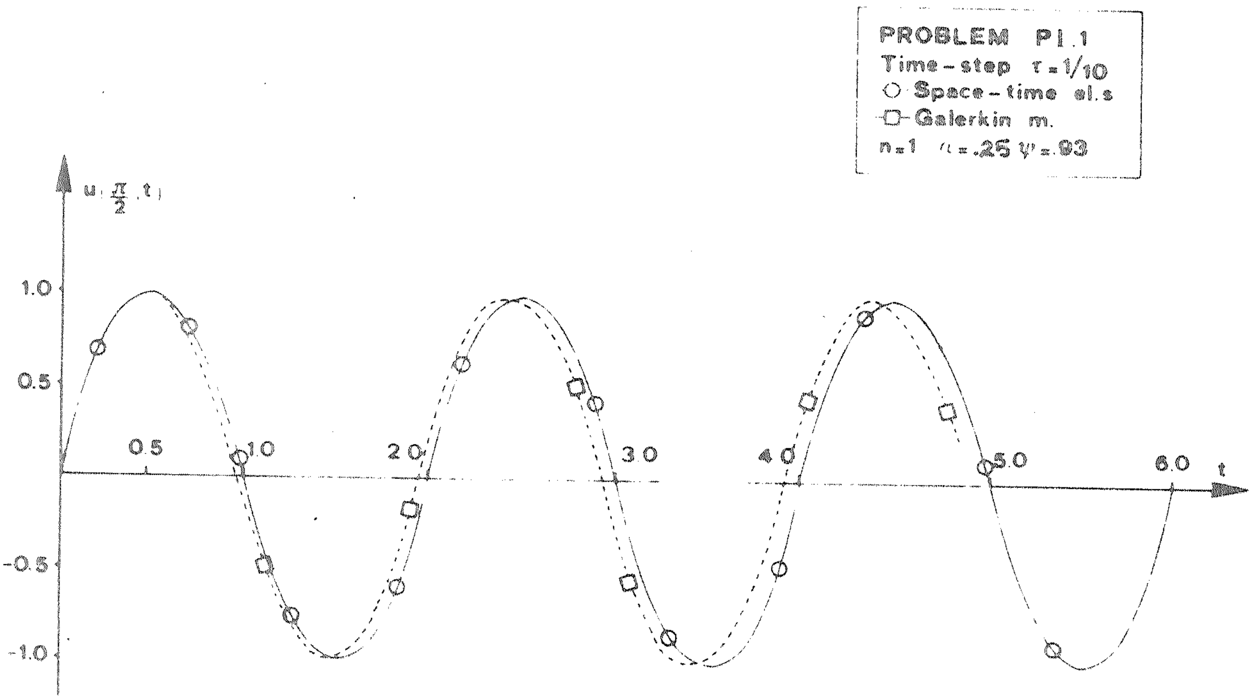

Fig. 20 - Test on linear hyperbolic.

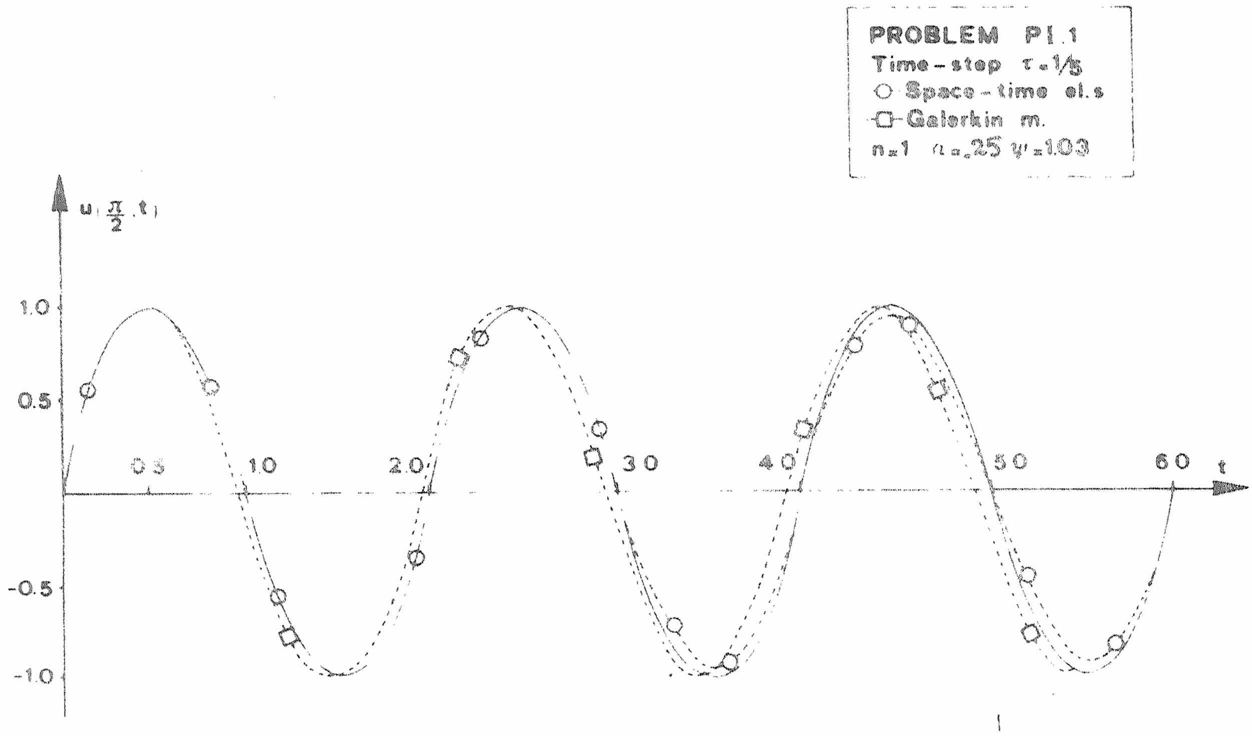

Fig. 21 - Test on linear hyperbolic.

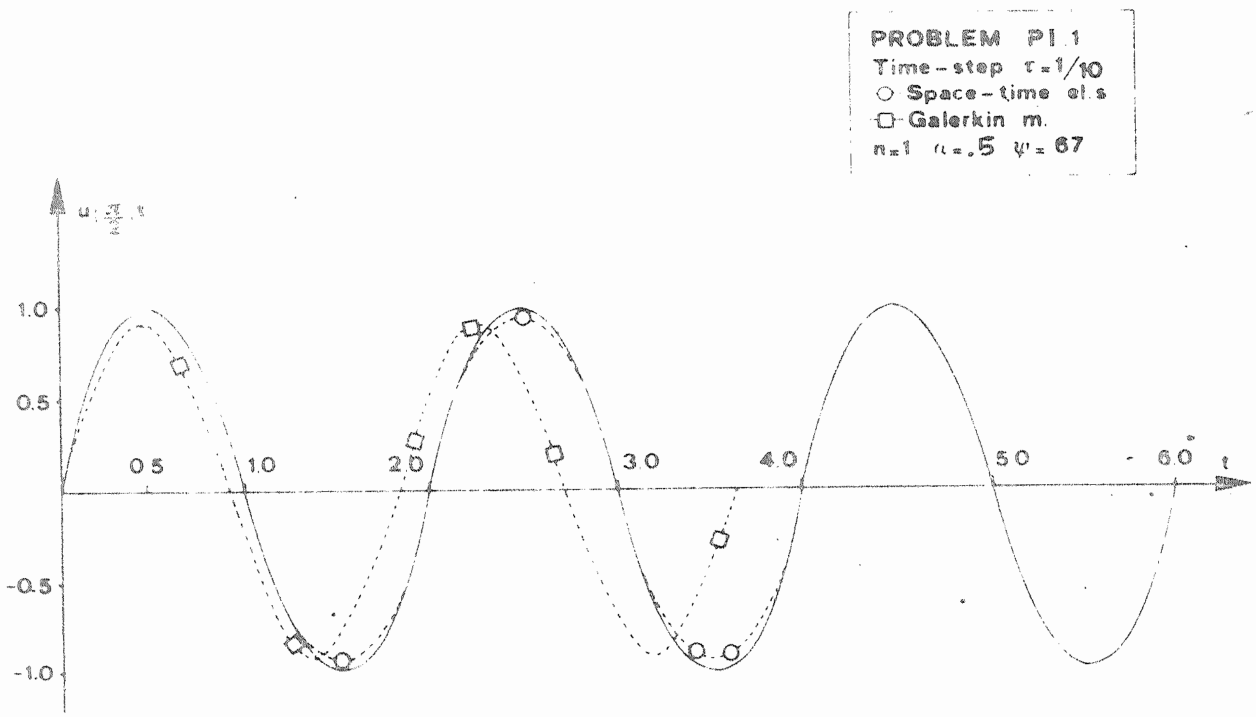

Fig. 22 - Test on linear hyperbolic.

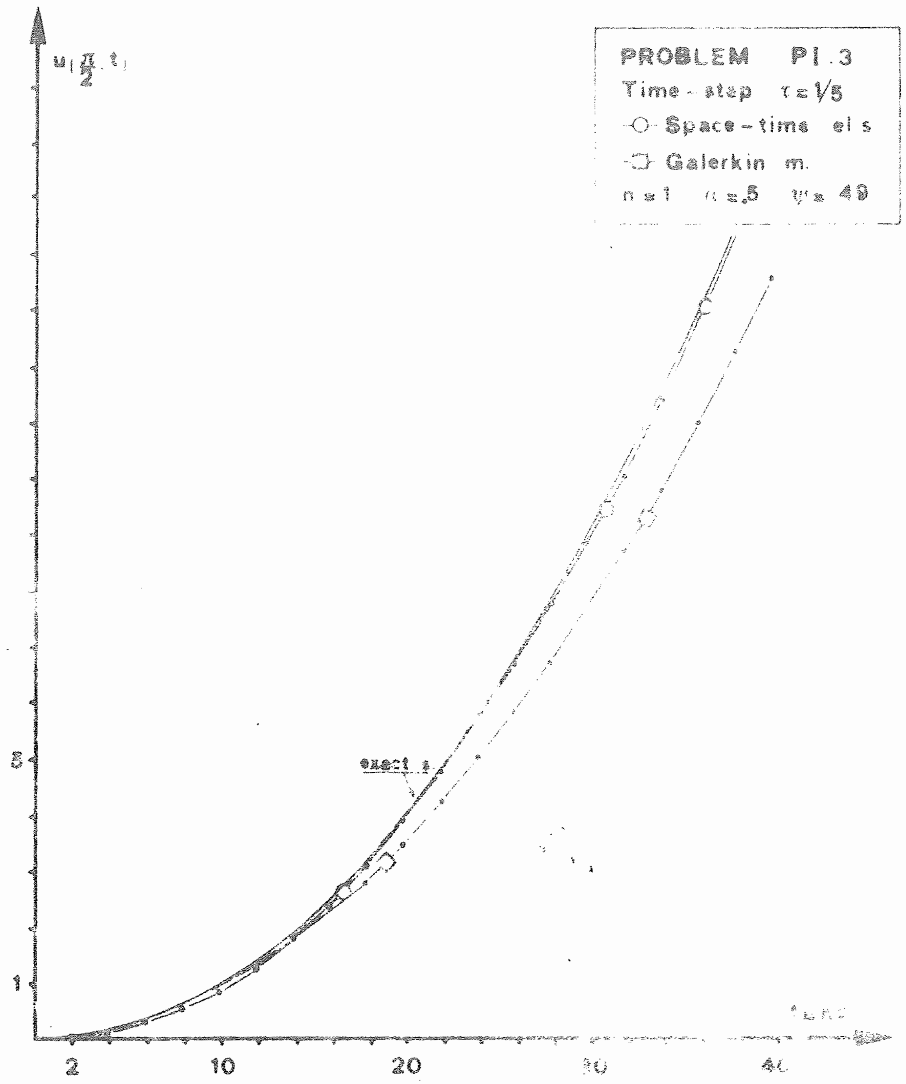

Fig. 25 - Test on hyperbolic with f(t)

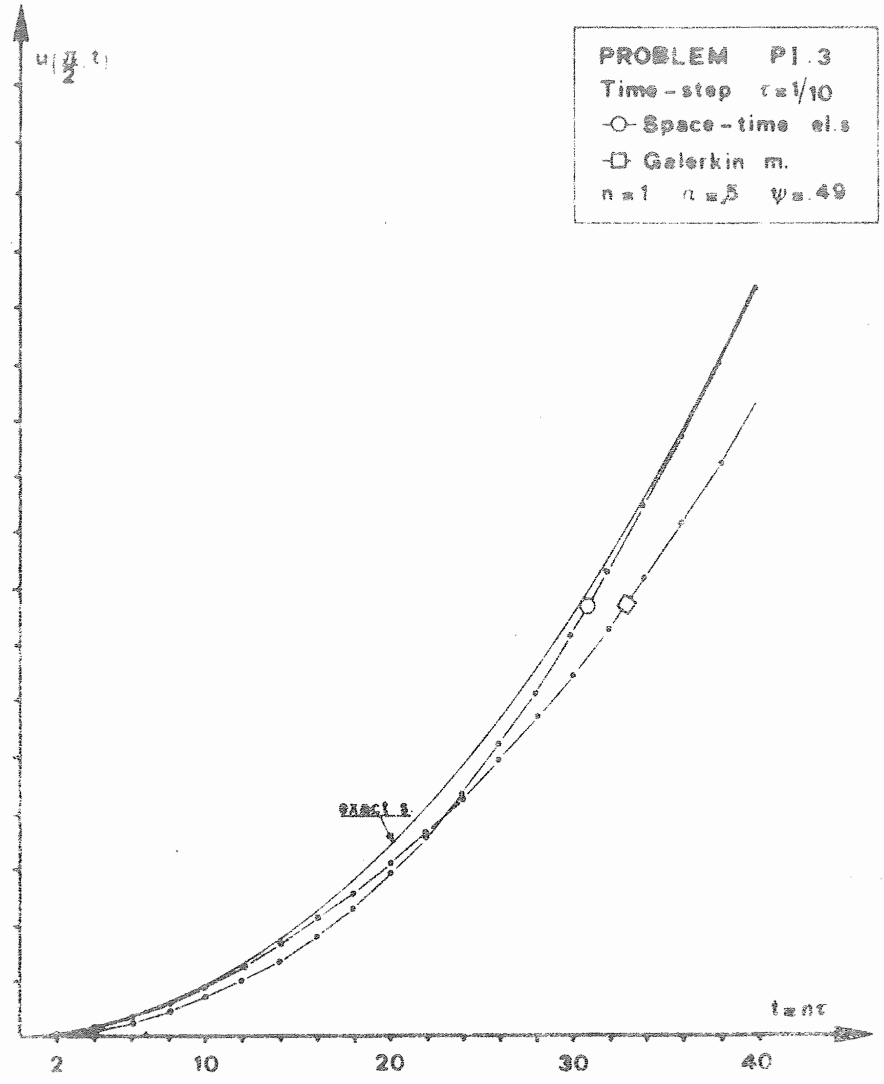

Fig. 26 - Test on hyperbolic with f(t)